EFFECTS OF PRESSURE GRADIENT/WALL VELOCITY SKEWNESS ON THE STABILITY OF COUETTE-POISEUILLE FLOWS

Muhammad Abdullah
Department of Mechanical Engineering & Applied Mechanics
University of Pennsylvania
Philadelphia, PA 19104, USA
muhabd@seas.upenn.edu

George Ilhwan Park
Department of Mechanical Engineering & Applied Mechanics
University of Pennsylvania
Philadelphia, PA 19104, USA
gipark@seas.upenn.edu

ABSTRACT

We describe a detailed numerical study of stability in the so-called oblique Couette-Poiseuille flows, which comprise simple examples of three-dimensional boundary layers. Through comparison with the Orr-Sommerfeld operator for the more familiar aligned case, we show that an effective wall speed completely characterizes modal stability. We leverage this to succinctly explain trends in the critical Reynolds number, which, at sufficiently large wall speeds, becomes exclusively dependent on the direction of wall motion. An analysis of transient growth reveals that three-dimensionality is detrimental to energy amplification, reminiscent of turbulent three-dimensional boundary layers, where a similar decline in the energy production is a commonly observed feature. The associated optimal perturbation is found to develop via a lift-up effect enhanced by an Orr-like mechanism.

INTRODUCTION

Current turbulence theories rely heavily on observations in flows that are, in a mean sense, two-dimensional. In contrast, many boundary layer flows are often *three-dimensional*, with skewed mean velocity vectors and flow angles that vary non-trivially with the wall-normal coordinate. Here, we systematically analyze the stability of a class of internal flows that generalize the traditional Couette-Poiseuille configuration by allowing for a misalignment – prescribed by an angle of skewness θ – between the pressure gradient and the wall velocity vectors. We refer to these as *oblique* Couette-Poiseuille flows (OCPfs), and cite wind-water interactions, turbo-machinery, tribology, and geo-physical flows as immediate applications.

Oblique Couette-Poiseuille flows have remained relatively underexplored in the literature, and, in fact, to the best of our knowledge, this work is the first to exhaustively investigate their linear stability. In contrast, the aligned case, $\theta = 0$, abbreviated hereafter as ACPf, has been studied more extensively, with Potter (1966) and Reynolds & Potter (1967) providing most of the initial work in this regard. Described by the non-dimensional wall speed ξ (typically scaled with the center-line maximum for simple Poiseuille flow), the parallel superposition of a Couette component is, in general, stabilizing, at least in terms of a critical Reynolds number Re_c below which eigenvalue instability is absent. Furthermore, beyond the threshold value $\xi \approx 0.7$, the base flow achieves complete linear stability against infinitesimal perturbations. Meanwhile, for non-modal disturbances, Bergström (2004) reported generally large algebraic growth, albeit heavily dependent on the relative influences of the Poiseuille versus Couette components.

Interestingly, studies on *turbulent* OCPfs appear to be more common, and in this community, these flows form prototypical examples of the so-called "viscous-induced" three-dimensional boundary layers. Unfortunately, however, almost all relevant work to date has focused exclusively on wall motion that is precisely orthogonal to the pressure gradient, $\theta = \pi/2$, with almost no attention devoted to intermediate regimes. Coleman *et al.* (1996) and Le *et al.* (2000), for example, examined the turbulent statistics of two-dimensional channel flows perturbed by impulsive (orthogonal) spanwise wall motion. Extending this work, Kannepalli & Piomelli (2000) displaced only a finite section of the wall so as to contrast the initial response of the flow with its subsequent relaxation to a two-dimensional equilibrium turbulence. A common theme within these investigations, and indeed within the general context of three-dimensional boundary layers, is the unusual reduction in turbulent stresses (and, by extension, turbulent energy production) relative to the two-dimensional case, which occurs despite the addition of mean shear (Moin *et al.*, 1990; Lozano-Durán *et al.*, 2020). Thus, it is of particular interest to see whether a similar phenomenon might remain relevant here.

PROBLEM FORMULATION

Figure 1 summarizes a typical OCPf. Here, the governing equations are standard for incompressible fluid flow

$$\frac{\partial \boldsymbol{u}}{\partial t} + (\boldsymbol{u} \cdot \nabla)\, \boldsymbol{u} = -\nabla p + \frac{1}{Re} \nabla^2 \boldsymbol{u} \tag{1}$$

and we non-dimensionalize length with the channel half-width h, velocity with the center-line value U_p for Poiseuille flow,

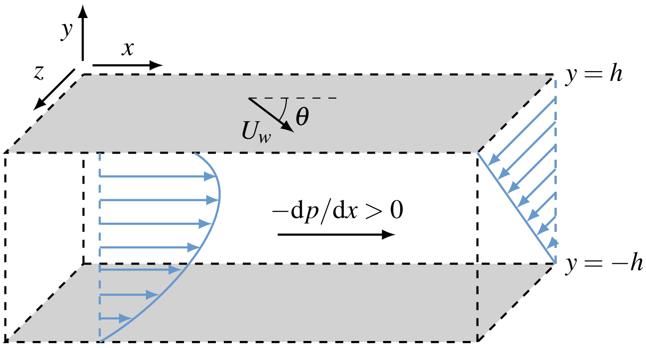

Figure 1. A sketch of the flow geometry for oblique Couette-Poiseuille flows. The wall at $y = h$ translates with a velocity U_w at an angle $\theta \neq 0$ to the streamwise direction, inducing a three-dimensional shear flow.

time with h/U_p, and the pressure with ρU_p^2, where ρ denotes the fluid density. The Reynolds number is $Re = U_p h/\nu$, where ν is the kinematic viscosity, and the base profile can be described by $\boldsymbol{U} = \left(U(y)\ 0\ W(y)\right)$, where

$$U(y) = 1 - y^2 + \frac{\xi}{2}(1+y)\cos\theta \tag{2}$$

$$W(y) = \frac{\xi}{2}(1+y)\sin\theta \tag{3}$$

and $\xi = U_w/U_p$ is the non-dimensional wall speed. Assuming now a set of infinitesimal fluctuations, we linearize Equation (1) around $\boldsymbol{U}$. Converting to a formulation involving perturbations in the wall-normal velocity/vorticity $\left(v'\ \eta'\right)$, we adopt a normal mode ansatz

$$\begin{pmatrix} v'(x,y,z,t) \\ \eta'(x,y,z,t) \end{pmatrix} = \boldsymbol{\chi} e^{i(\alpha x + \beta z)} \qquad \boldsymbol{\chi} = \begin{pmatrix} \overline{v}(y,t) \\ \overline{\eta}(y,t) \end{pmatrix} \tag{4}$$

which yields a system of the form

$$\mathsf{L}\boldsymbol{\chi} = -\frac{\partial}{\partial t}\mathsf{M}\boldsymbol{\chi} \implies \frac{\partial \boldsymbol{\chi}}{\partial t} = \mathsf{S}\boldsymbol{\chi} \tag{5}$$

Here, denoting $\mathsf{D} \equiv \mathrm{d}/\mathrm{d}y$ and $k^2 = \alpha^2 + \beta^2$, we have defined

$$\mathsf{L} = \begin{pmatrix} \mathsf{L}_{\mathsf{OS}} & 0 \\ i\beta \mathsf{D}U - i\alpha \mathsf{D}W & \mathsf{L}_{\mathsf{SQ}} \end{pmatrix} \qquad \mathsf{M} = \begin{pmatrix} \mathsf{D}^2 - k^2 & 0 \\ 0 & 1 \end{pmatrix} \tag{6}$$

where the *Orr-Sommerfeld* and *Squire* operators, L_{OS} and L_{SQ} respectively, are given by

$$\begin{aligned} \mathsf{L}_{\mathsf{OS}} = {} & (i\alpha U + i\beta W)(\mathsf{D}^2 - k^2) \\ & - i\alpha \mathsf{D}^2 U - i\beta \mathsf{D}^2 W - \frac{1}{Re}(\mathsf{D}^2 - k^2)^2 \end{aligned} \tag{7}$$

$$\mathsf{L}_{\mathsf{SQ}} = i\alpha U + i\beta W - \frac{1}{Re}(\mathsf{D}^2 - k^2) \tag{8}$$

The spectrum $\Lambda(\mathsf{S})$ dictates the stability of the system in Equation (5), and for asymptotic stability, we require $\lambda_r < 0$ for $\lambda = \lambda_r + i\lambda_i \in \Lambda(\mathsf{S})$. The manifold of neutral growth is then given by

$$\lambda_r(\alpha, \beta, Re, \xi, \theta) = 0 \tag{9}$$

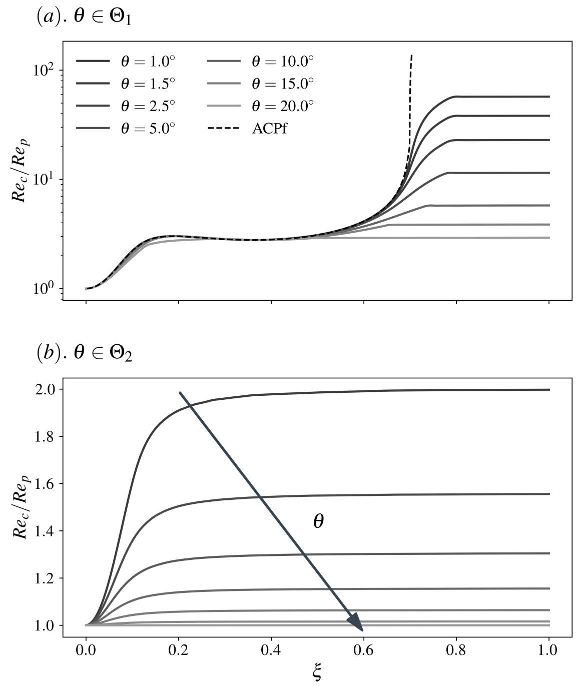

Figure 2. The critical Reynolds number Re_c, normalized with the equivalent value Re_p for Poiseuille flow ($\xi \to 0$), for angles θ in (a), Θ_1 and (b), Θ_2. In the second panel, the arrow denotes the direction of increasing θ from $\theta = 30^\circ$ to $\theta = 90^\circ$ in increments of 10°.

However, since the stability equations for shear flows are typically non-self-adjoint, S is, in general, highly non-normal (Trefethen *et al.*, 1993). Thus, one must account for the possibility of finite-time non-modal energy growth that cannot be quantified purely by a spectral analysis. Here, we consider the gain G of the state transition operator $\Phi(t,0)$ for the linear system in Equation (5). We adopt the energy norm $\|\cdot\|_E$, where

$$\|\boldsymbol{\chi}\|_E^2 = \int_{-1}^{1} \overline{v}^\dagger \overline{v} + \frac{1}{k^2}\left(\overline{\eta}^\dagger \overline{\eta} + \frac{\partial \overline{v}^\dagger}{\partial y}\frac{\partial \overline{v}}{\partial y}\right) \mathrm{d}y \tag{10}$$

so that $G = \|\Phi(t,0)\|_E^2$ can be computed via a weighted singular value decomposition. Physically, this gain represents an optimization of the energy amplification at time t over all possible initial states having unit norm; see Schmid & Henningson (2001) for more information. Our numerical experiments were conducted in `Python` using a standard Chebyshev pseudospectral method, and we scaled our parameter sweeps using the open-source module `Ray` (Moritz *et al.*, 2018).

MODAL ANALYSIS

First, we summarize an investigation of modal stability in OCPfs. We begin by introducing the critical Reynolds number Re_c, which represents the minimum Reynolds number below which the flow remains asymptotically stable, $\lambda_r < 0$. The associated critical wavenumbers are defined as (α_c, β_c), and evoke a neutrally stable mode, $\lambda_r = 0$. Thus, beyond this threshold, at least one disturbance must become unstable, that is, $\lambda_r > 0$. Since OCPfs are not amenable to Squire's Theorem, the spanwise wavenumber β becomes a relevant stability parameter and cannot be set to zero *a priori*. On the other hand, the Squire modes remain damped as in the case

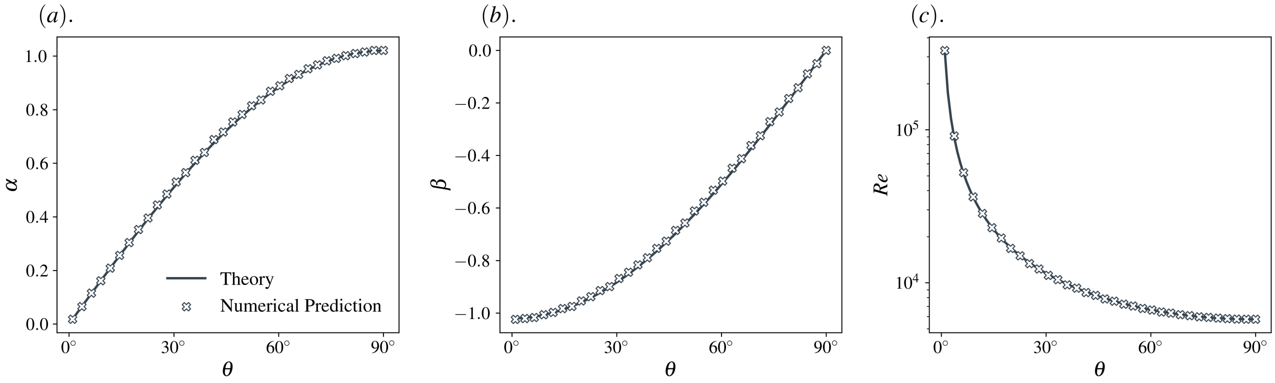

Figure 3. The asymptotic values of (*a*–*b*), the critical streamwise and spanwise wavenumbers and (*c*), the critical Reynolds number versus θ. The solid lines denote the theoretical estimates derived from Equation (13).

of two-dimensional flows, and it suffices to consider only the Orr-Sommerfeld operator when investigating modal stability.

We limit our attention to pairs $(\xi,\theta) \in [0,1] \times [0°,90°]$. For various OCPf configurations, Figure 2 provides plots of Re_c normalized with the critical Reynolds number for Poiseuille flow, $Re_p \approx 5772.73$ (Schmid & Henningson, 2001). Two regimes of interest can be identified, demarcated, respectively, as $\Theta_1 \equiv (0,20°]$ and $\Theta_2 \equiv (20°,90°]$. Within the former, a typical Re_c-curve is qualitatively similar to that for ACPf: a short range of stabilization is followed by an inflection point and then further growth. We see that increasing obliqueness is, in general, destabilizing (relative to ACPf), an effect that is prevalent even in Θ_2. In the latter regime, we also note a stronger departure from the stability features of ACPfs, as evidenced, for example, by the Re_c-curves forgoing their inflectional nature. Interestingly, we see in Figure 2 that non-trivial ($\theta \neq 0$) OCPfs remain linearly unstable for all wall speeds explored here. This is evidently in stark contrast to ACPf, which is well-known to become unconditionally linearly stable after the so-called “cut-off” $\xi \approx 0.7$ (Potter, 1966). Furthermore, regions of ξ-space appear to emerge where Re_c (and the associated critical wavenumbers, not shown here) approach asymptotic values; in other words, *the flow stability becomes independent of the strength of wall motion for sufficiently large* ξ. This is most pronounced for $\theta = 90°$, for which the critical triplet at *all* ξ is found to be exactly the same as for the Poiseuille flow, $\xi = 0$, that is,

$$(\alpha_c,\beta_c,Re_c)_{\theta=90°} \approx \left(\alpha_p,\beta_p,Re_p\right) = (1.02,0,5772.73) \quad (11)$$

By extension, the streamwise and wall-normal component of the associated eigen-function also precisely match those of the Poiseuille Tollmien-Schlichting wave (with the addition of a non-zero spanwise component, however, due to the mean spanwise shear).

In order to rationalize these observations, we first note that $\mathsf{D}^2W = 0$, so that the Orr-Sommerfeld operators for OCPf and ACPf can be made equivalent by defining

$$\xi_{\text{eff}}\left(\alpha,\beta,Re,\xi\right) = \xi\left(\cos\theta + \frac{\beta}{\alpha}\sin\theta\right) \quad (12)$$

as an “effective” wall speed for the aligned problem. The immediate consequence is that the stability of any OCPf can be fully characterized by comparison with the appropriate ACPf configuration(s). In particular, Potter (1966) showed that ACPfs are most unstable (in the sense of Re_c) when $\xi \to 0$, that is, in the limit of the Poiseuille flow. Therefore, to “maximize” destabilization, the Orr-Sommerfeld problem for OCPfs at criticality must degenerate into the two-dimensional analog for Poiseuille flow, that is, following an application of Squire's Theorem. This will happen if and only if

$$\xi_{\text{eff}} = 0 \qquad \alpha^2+\beta^2 = \alpha_p^2 \qquad \alpha Re = \alpha_p Re_p \quad (13)$$

The system in Equation (13) can be solved exactly (assuming non-negative α) and Figure 3 highlights that these theoretical values agree excellently with our numerical findings for the asymptotic critical parameters (notice, in particular, that the prediction for $\theta = 90°$ in Figure 3 matches Equation (11)). An intriguing implication of this analysis arises for the asymptotic eigen-function; specifically, in wave theory, the direction of wave motion is encoded within the wavenumber vector $\boldsymbol{k} = \begin{pmatrix}\alpha & \beta\end{pmatrix}$ so that a wave with wavenumber vector $\boldsymbol{k}$ will propagate at an angle ψ to the positive streamwise direction, where $\tan\psi = \beta/\alpha$. From the first expression in Equation (13), it is then possible to conclude that the asymptotic eigenmode propagates at an angle $\psi = \theta - \pi/2$ to the pressure gradient, that is, exactly perpendicular to the wall motion.

TRANSIENT GROWTH ANALYSIS

We now focus on the potential for transient (algebraic) energy growth in the initial-value problem, Equation (5). For an arbitrary OCPf configuration (ξ,θ), we consider $G_{\max}$, defined as the output of the following optimization

$$G_{\max}\left(Re,\xi,\theta\right) = \max_{\alpha,\beta,t} G\left(\alpha,\beta,Re,\xi,\theta,t\right) \quad (14)$$

Thus, physically, $G_{\max}$ represents the maximal amplification admissible across time and wavenumber space. Figure 4 outlines the findings of a large parameter sweep for $G_{\max}$ at $Re = 1000$. For simple ACPf, we immediately observe a monotonic increase in $G_{\max}$ with ξ. The introduction of a weak misalignment maintains this trend, even allowing marginally greater amplification throughout the full range of wall speeds, an effect that evidently peaks at $\theta = 4.5°$. At even larger angles of skewness, two different regimes can be identified. In particular, while $G_{\max}$ continues to grow with θ, albeit nominally, for

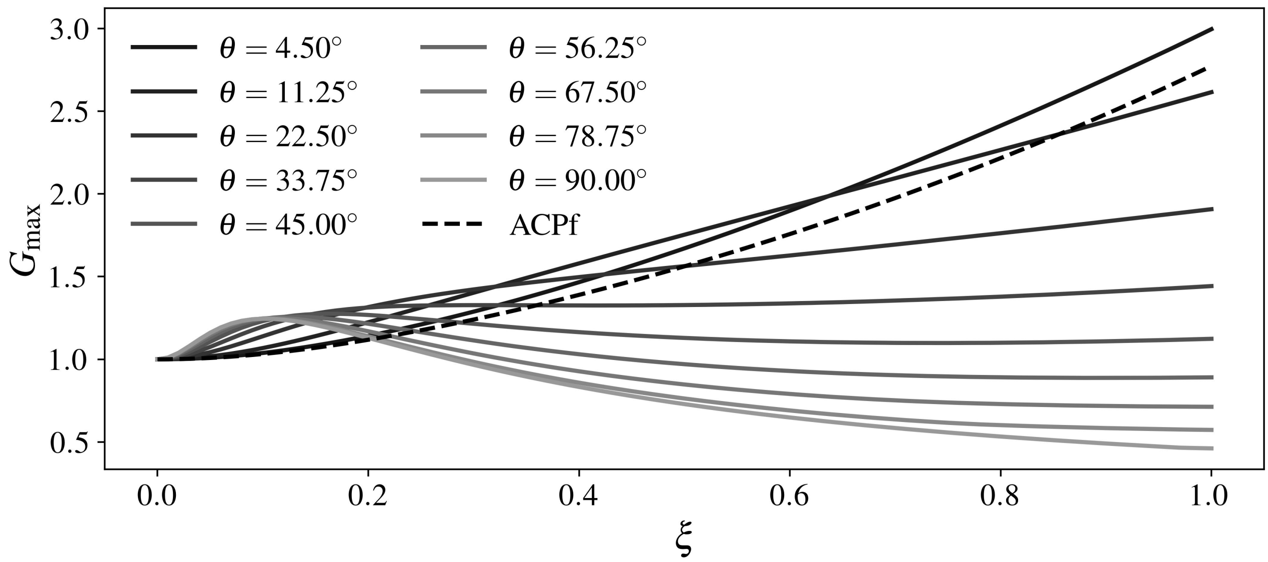

Figure 4. Curves of $G_{\max}$, the maximal energy gain experienced by OCPfs across time and wavenumber space, for some representative θ. All values have been normalized with $G_{\max}(\xi = 0) \approx 196$. A dashed line indicates ACPf, $\theta = 0$. The largest amplification is generally realized for small but non-zero angles, most notably for $\theta \approx 4.5°$. At high levels of obliqueness, energy amplification evidently suffers, particularly for modest to large wall speeds.

$0 < \xi \lessapprox 0.15$, it decreases quite rapidly for $\xi \geq 0.2$. Furthermore, no "asymptotic" behavior akin to our modal results was resolved for $G_{\max}$.

Interestingly, within the framework of unforced algebraic growth, it is evident that a greater degree of misalignment is typically more "stable", with $\theta = 90°$ providing the strongest reduction in $G_{\max}$ for a wide range of wall speeds. Of course, this sharply contradicts the predictions of the earlier eigenvalue analysis, which claims that a perfectly orthogonal OCPf, in fact, minimizes Re_c in the (ξ, θ)-plane. Thus, on the finite time scales along which transient mechanisms operate, an antagonistic effect suppressing non-modal energy growth seems to be at play. This is especially notable since, individually, both the ACPf and the standard Couette flow support strong transient responses, yet for sufficiently skewed OCPfs, $G_{\max}$ can drop to as low as 46% of the equivalent value for the Poiseuille flow ($G_{\max} \approx 196$) at this Reynolds number.

Such a dampening of the perturbation energy is remarkably reminiscent of fully turbulent three-dimensional boundary layers, where increasing skewness is known to similarly impair the production of turbulent kinetic energy, despite the addition of a secondary source of shear. Numerous hypotheses have attempted to explain this phenomenon, and the most typical explanation suggests a deviation of momentum-carrying eddies from their "optimal" alignment by the mean spanwise strain (Bradshaw & Pontikos, 1985). In the context of laminar OCPfs, as treated here, such an ideal configuration can potentially be quantified by considering the θ maximizing $G_{\max}$ at a given ξ, here denoted as $\theta_{\max}$. Figure 5(a) illustrates that this quantity decays primarily as a power law, but what is more important is that the associated cross-stream component W is quite weak, as highlighted in Figure 5(b). In a similar vein, the flow direction ϕ, defined as

$$\phi = \arctan\left(\frac{W(y)}{U(y)}\right) \tag{15}$$

and plotted in Figure 5(c), also generally collapses throughout most of the channel, experiencing rapid variation only near the upper wall. This is further emphasized in the inset provided in the same panel, which shows the average skewness $\widetilde{\phi}$, where

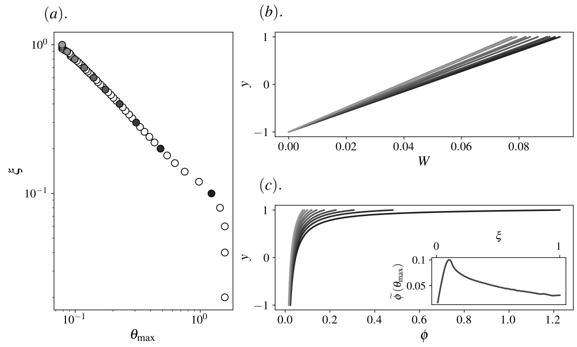

Figure 5. (a), the variation in ξ of $\theta_{\max}$, the angle maximizing $G_{\max}$. For select pairs of $(\xi, \theta_{\max})$, the associated crossflow and flow angle profiles have been highlighted with the appropriate color in (b) and (c), respectively. An inset in (c) shows the y-averaged deviations $\widetilde{\phi}$ from the streamwise direction; see Equation (16).

$$\widetilde{\phi} = \frac{\int_{-1}^{1} \phi(y)\,\mathrm{d}y}{\int_{-1}^{1} \mathbf{1}\,\mathrm{d}y} = \frac{1}{2}\int_{-1}^{1} \phi(y)\,\mathrm{d}y \tag{16}$$

We see that $\widetilde{\phi}$ remains small ($\approx 6°$ at worse) for all ξ. Thus, the optimal configuration appears to be roughly universal in ξ, comprising what is effectively a collateral boundary layer with an approximately constant flow direction in y.

At $\xi = 0.25$, Figure 6 presents for various θ the initial condition that realizes $G_{\max}$ as well as the associated response field at the optimal time. In two-dimensional flows such as ACPf, this energy-optimal pair is characterized by weak counter-rotating streamwise vortices, infinitely elongated in

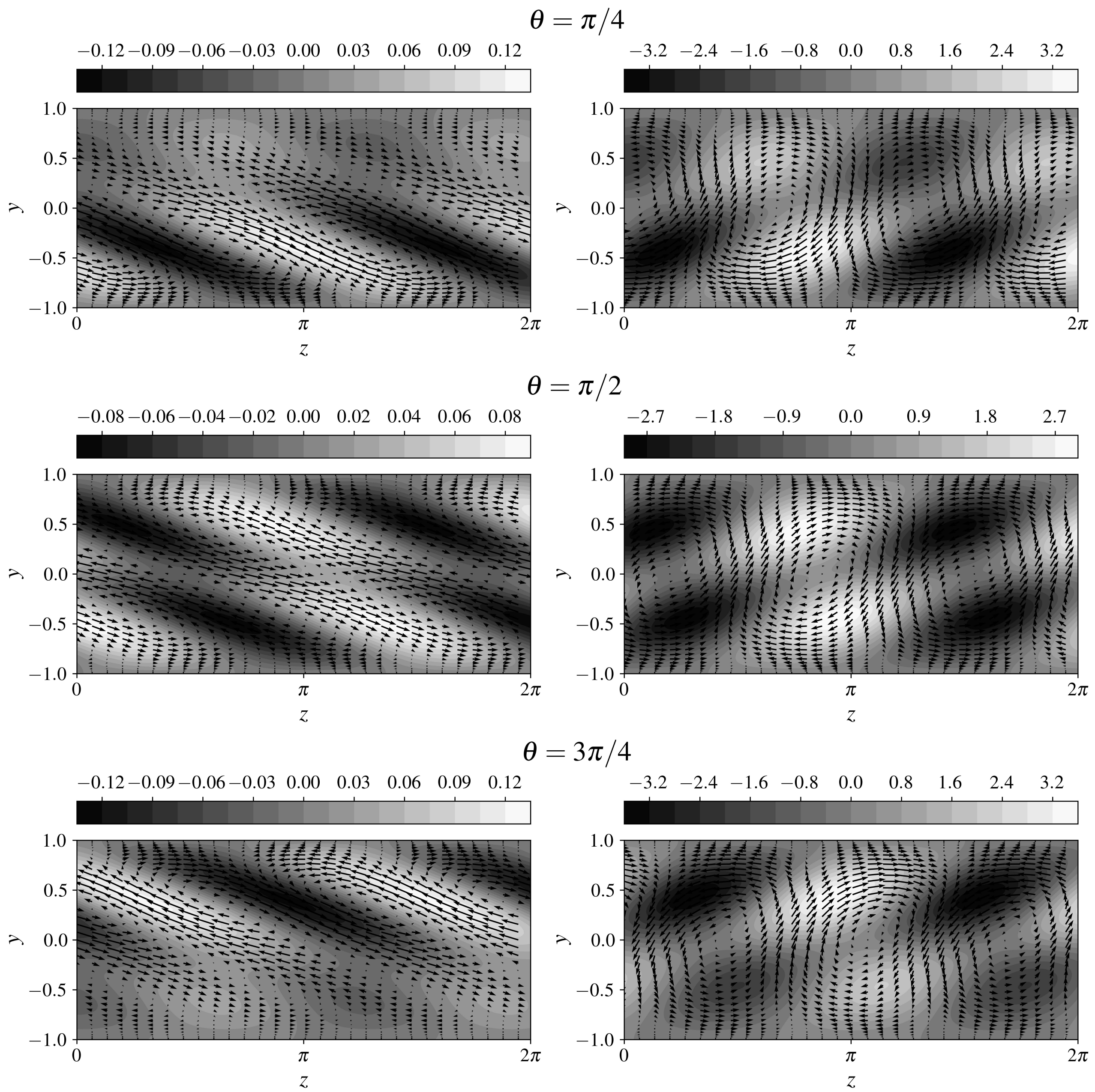

Figure 6. The optimal initial condition (left) and response at optimal time (right) for some values of θ at $\xi = 0.25$. The color and quiver arrows represent, respectively, the streamwise and cross-stream velocity perturbations.

the streamwise direction, that intensify through a redistribution of mean momentum by the wall-normal perturbations. Originally proposed by Ellingsen & Palm (1975), this process is commonly referred to as the lift-up effect, in which a linear amplification in time proportional to the streamwise shear can be achieved for a streamwise-independent disturbance, at least to the linear order when viscosity is taken into account. Although the three-dimensionality of our flow introduces additional nuance, Ellingsen & Palm (1975) had suggested that the lift-up process could remain viable even in skewed boundary layers, arguing, however, that streak growth would substantially decrease, particularly in the case of OCPfs because the streamwise shear itself decreases as θ approaches exact orthogonality.

Therefore, it is not surprising that the optimal initial conditions in Figure 6 comprise weak streamwise vortices whose amplification at the optimal time decreases in response to an increase in flow obliqueness, consistent with Figure 4. However, as captured by both Blesbois *et al.* (2013) and Hack & Zaki (2015) for their base flows, these vortices also initially oppose and eventually tilt in the direction of the *spanwise mean shear*, analogous to the classic down-gradient mechanism proposed by Orr (1907). Interestingly, then, because we can expect the crossflow to only enhance the additional non-modal energy gain provided by this process, it is likely that the trends observed in Figure 4 are a consequence of a decrease in the overall effectiveness of the lift-up process.

CONCLUSIONS

We have performed a comprehensive parameter sweep exploring modal and non-modal stability in oblique Couette-Poiseuille profiles. By introducing an angle of skewness θ between the pressure gradient and the wall velocity vectors, these flows generalize the more commonly explored ACPfs, $\theta = 0$. We show that this misalignment is generally destabilizing, at least as far as Re_c is concerned. Furthermore, it is found that criticality eventually becomes a function of only the direction of wall movement (that is, θ), which is explained by identifying an effective wall speed that maps the stability equations to those for ACPf. The exact values of the critical parameters are thence derived in this asymptotic regime and shown to agree well with our numerical findings. Separately, algebraic growth is determined to be highly suppressed as θ increases, replicating the energy dampening prevalent in *turbulent* three-dimensional boundary layers. In a similar vein, the base flow configuration that maximizes the energy gain at any wall speed ξ is found to be an approximately collateral – effectively two-dimensional – boundary layer. Finally, the most energetic initial perturbations seem to develop via a lift-up process enhanced by an Orr-like mechanism, the latter arising from the cross-stream shear.

REFERENCES

Bergström, Lars B. 2004 Nonmodal growth of three-dimensional disturbances on plane Couette–Poiseuille flows. *Physics of Fluids* **17**.

Blesbois, Olivier, Chernyshenko, Sergei I., Touber, Emile & Leschziner, Michael A. 2013 Pattern prediction by linear analysis of turbulent flow with drag reduction by wall oscillation. *Journal of Fluid Mechanics* **724**, 607–641.

Bradshaw, P. & Pontikos, N. S. 1985 Measurements in the turbulent boundary layer on an 'infinite' swept wing. *Journal of Fluid Mechanics* **159**, 105–130.

Coleman, Gary N., Kim, John & Le, Anh-Tuan 1996 A numerical study of three-dimensional wall-bounded flows. *International Journal of Heat and Fluid Flow* **17** (3), 333–342.

Ellingsen, T. & Palm, E. 1975 Stability of linear flow. *The Physics of Fluids* **18** (4), 487–488.

Hack, M. J. Philipp & Zaki, Tamer A. 2015 Modal and non-modal stability of boundary layers forced by spanwise wall oscillations. *Journal of Fluid Mechanics* **778**, 389–427.

Kannepalli, Chandrasekhar & Piomelli, Ugo 2000 Large-eddy simulation of a three-dimensional shear-driven turbulent boundary layer. *Journal of Fluid Mechanics* **423**, 175–203.

Le, Anh-Tuan, Coleman, Gary N. & Kim, John 2000 Near-wall turbulence structures in three-dimensional boundary layers. *International Journal of Heat and Fluid Flow* **21** (5), 480–488, turbulence and Shear Flow Phenomena 1.

Lozano-Durán, Adrián, Giometto, Marco G., Park, George Ilhwan & Moin, Parviz 2020 Non-equilibrium three-dimensional boundary layers at moderate reynolds numbers. *Journal of Fluid Mechanics* **883**, A20.

Moin, P., Shih, T.-H., Driver, D. & Mansour, N. N. 1990 Direct numerical simulation of a three-dimensional turbulent boundary layer. *Physics of Fluids A: Fluid Dynamics* **2** (10), 1846–1853.

Moritz, Philipp, Nishihara, Robert, Wang, Stephanie, Tumanov, Alexey, Liaw, Richard, Liang, Eric, Elibol, Melih, Yang, Zongheng, Paul, William, Jordan, Michael I. & Stoica, Ion 2018 Ray: A distributed framework for emerging ai applications. p. 561–577. USA.

Orr, William M'F. 1907 The stability or instability of the steady motions of a perfect liquid and of a viscous liquid. part ii: A viscous liquid. *Proceedings of the Royal Irish Academy. Section A: Mathematical and Physical Sciences* **27**, 69–138.

Potter, Merle C. 1966 Stability of plane Couette–Poiseuille flow. *Journal of Fluid Mechanics* **24** (3), 609–619.

Reynolds, W. C. & Potter, Merle C. 1967 Finite-amplitude instability of parallel shear flows. *Journal of Fluid Mechanics* **27** (3), 465–492.

Schmid, P.J. & Henningson, D.S. 2001 *Stability and Transition in Shear Flows*. *Applied Mathematical Sciences* 1. Springer New York.

Trefethen, Lloyd N., Trefethen, Anne E., Reddy, Satish C. & Driscoll, Tobin A. 1993 Hydrodynamic stability without eigenvalues. *Science* **261** (5121), 578–584.